Journal of Membrane Science and Research 7 (2021) 74-84

Journal of Membrane Science & Research

journal homepage: www.msrjournal.com

Research Paper

Effect of 2-MeIM/Zn Molar Ratio on CO_2 Permeability of Pebax/ZIF-8 Mixed Matrix Membranes

Jeein Kim, Taejun Park, Eunhyea Chung *

Department of Energy System Engineering, Seoul National University, Gwanak-ro 1, Gwanak-gu, Seoul, 08826, Republic of Korea

Article info

Received 2019-12-24
Revised 2020-03-27
Accepted 2020-03-27
Available online 2020-03-27

Keywords

Pebax 1657
Pebax 2533
Controlling molar ratio of ZIF-8 precursors
Mixed matrix membranes
CO_2 capture

Highlights

- ZIF-8 nanoparticles size was controlled by molar ratio of ZIF-8 precursors
- CO_2 permeability of Pebax1657/ZIF-8 MMM was improved by smaller ZIF-8 nanoparticles
- CO_2 permeability of Pebax2533/ZIF-8 MMM was improved by larger ZIF-8 nanoparticles
- CO_2/N_2 selectivity was higher in Pebax 1657 MMMs than 2533 MMMs

Graphical abstract

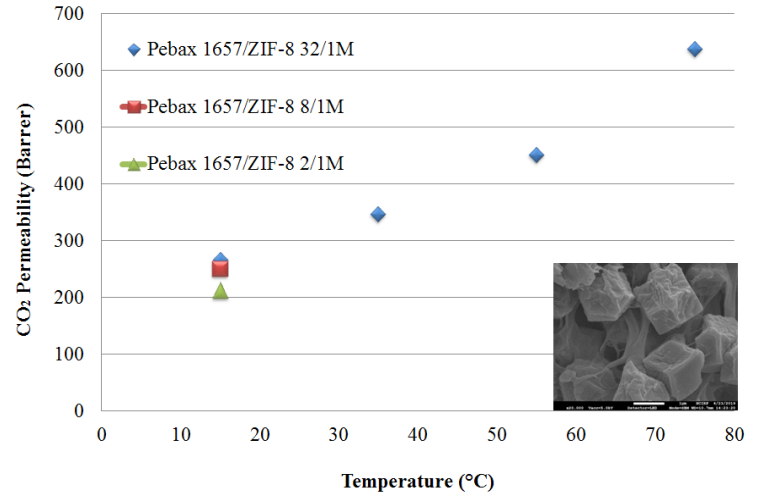

Abstract

The impact of controlling molar ratio of ZIF-8 precursors on Pebax 1657 and Pebax 2533 based Mixed Matrix Membranes (MMMs) on the CO_2 permeability and CO_2/N_2 ideal selectivity was investigated. Three types of ZIF-8 were synthesized by controlling molar ratio of 2-methylimidazole and zinc nitrate hexahydrate as 2/1, 8/1, and 32/1. The SEM images and XRD patterns of ZIF-8 showed that particle sizes and crystallinity peaks were decreased as molar ratio of ZIF-8 increased. The CO_2 permeability of Pebax MMM was improved by filling with the ZIF-8 particles compared to the pure Pebax. At equivalent temperatures, the highest CO_2 permeability was shown in Pebax 1657/ZIF-8 with the ZIF-8 precursors' molar ratio of 32/1 and Pebax 2533/ZIF-8 with the molar ratio of 2/1. As molar ratio of ZIF-8 precursors increases, CO_2 permeability of Pebax 1657 was increased by excessive sorption of CO_2 by imidazolium ions in ZIF-8, whereas CO_2 permeability of Pebax 2533 was decreased by decreasing pore size and particle size of ZIF-8. The CO_2 permeability was higher in Pebax 2533/ZIF-8 compared to Pebax 1657/ZIF-8, because Pebax 2533 has more concentrations of polar groups in the polymer matrix than Pebax 1657. However, the CO_2/N_2 ideal selectivity was higher in Pebax 1657/ZIF-8 compared to Pebax 2533/ZIF-8 because diffusivity of Pebax 1657 compared to Pebax 2533 is lower for nonpolar gases, such as N_2, and the solubility is higher for polarizable gases like CO_2. As increasing temperature, Pebax/ZIF-8 MMMs showed enhancement of CO_2 and N_2 permeability but decreased in CO_2/N_2 ideal selectivity.

1. Introduction

The use of fossil fuels has increased the concentration of gaseous CO_2 in the atmosphere, which has contributed to the greenhouse effect [1-4]. CO_2 can be captured using various mixtures, such as natural gas or flue-gas, through conventional technologies like absorption with solvents and cryogenic CO_2 capture [3]. However, these methods are being replaced by membrane technologies because of their low cost and energy-efficiency [1,2]. Generally, polymeric membranes have been applied to gas separation processes in industry because they consume low energy, have low cost, and are environmentally sustainable [3].

Recent studies have reported that the incorporation of a poly(ether oxide) (PEO) segment with other monomers can be used to overcome the weakness of fragile PEO segments to improve the weak mechanical strength [4,5]. Polyether block polyamide copolymers (Pebax) are widely studied for CO_2 separation because they are flexible, durable, and mechanically and thermally resistant. Furthermore, they show high selectivity of CO_2 over nonpolar gases such as N_2 and CH_4 [6,7]. Pebax is composed of a thermoplastic polyamide (PA) segment and rubbery polyether (PE) segment [7]. PA is a rigid and hard crystalline phase that provides mechanical strength to a Pebax membrane [8,9]. PE is a flexible and soft amorphous phase that provides high CO_2 permeability through its high affinity for polarizable molecules, which makes

* Corresponding author: echung@snu.ac.kr (E. Chung)

DOI: 10.22079/JMSR.2020.119041.1316

it feasible to select polarizable gases from nonpolar gases like N_2 [10].

The Robeson upper bound represents the empirical relationship between the permeability of a specific component of a gas mixture and its separation factor, defined by Lloyd M. Robeson [11]. As the separation factor decreases, the permeability of more permeable gas components increases [11]. Therefore, there is a trade-off relationship between permeability and selectivity, which the CO_2 permeability increases for polymeric membranes such as Pebax, while the CO_2 selectivity decreases [11]. This drawback of polymeric membranes can be overcome by combining highly permeable polymers with inorganic fillers, which can increase gas selectivity while maintaining high permeability for CO_2 [12].

To improve the permeability and mitigate the loss of selectivity, inorganic fillers are dispersed in polymeric membranes to produce hybrid membranes called mixed matrix membranes (MMMs) [3,7]. The fillers include zeolites, carbon molecular sieves, and inorganic particles like silica and TiO_2. However, conventional inorganic fillers have weak adhesion with organic polymers [1]. For sustainable production of MMMs, metal organic frameworks (MOFs) have been introduced as porous materials composed of metal ions linked to organic linkers, which provide high surface area that adsorbs affinitive gas molecules [1,12].

Zeolitic imidazolate frameworks (ZIFs) are a subclass of MOFs, which include zinc metal cations and 2-methylimidazole anions of organic linkers that form a six-membered ring [3]. ZIFs have a special molecular sieving effect that provides strong interfacial interaction with polymers [13-16]. ZIFs are used as a membrane supplement for CO_2 capture as they have high thermal and chemical stability, and their micro-pore size of 3.4 Å is suitable for gas transport of CO_2, which has a kinetic diameter of 3.3 Å [6,17,18]. ZIF-8 particles are well connected to Pebax by forming hydrogen bonds between methyl groups in ZIF-8 and aldehyde in Pebax or between N atoms on imidazole in ZIF-8 and N-H groups in Pebax [12]. This makes permeation easier for polarizable CO_2 gas molecules because extra hydrogen bonds between PA segment and ZIF-8 make interactions between polymer and ZIF-8 nanoparticles more rigid and stabilized [12,19,20].

Even though ZIF-8 based Pebax MMMs have shown enhanced CO_2 permeability compared to pure Pebax, increasing the amount of ZIF-8 particles leads to lower CO_2 selectivity over other gases [6,20,22]. This is due to micro-phase separation that occurs in the Pebax/ZIF-8 MMMs, which creates more free volume and can improve permeability of both CO_2 and N_2 [6]. To improve the CO_2 selectivity, better interface compatibility is needed between the inorganic ZIF-8 filler and the organic polymer Pebax membrane [7]. To achieve interfacial volume without defects in MMMs, the molar ratio-controlling technique for the precursor of inorganic filler has been modified for membrane fabrication.

Jomekian et al. [7] modified Pebax 1657/ZIF-8 MMMs by increasing molar ratios of ZIF-8 precursors with decreasing particle size and used ionic liquids on the surface of MMMs. The CO_2 permeability of pure Pebax 1657 was 150 Barrer, which increased to 250, 275, and 290 Barrer as the ZIF-8 particle size decreased. As higher molar ratio of ZIF-8 precursors increases interfacial area between particle and polymer, fractional free volume increases which directly increases the permeability. Furthermore, the CO_2/N_2 selectivity was consistently increased and changed only slightly with the decrease of ZIF-8 particles. In contrast, other studies showed that the selectivity of CO_2/N_2 decreased when simply increasing the ZIF-8 loading [3,6].

Sánchez-Laínez et al. [23] synthesized ZIF-8 nanoparticles with sizes of 50, 70, and 150 nm for use in a polybenzimidazole matrix to perform CO_2 and H_2 permeation tests. The particles enhanced the CO_2 permeability, and the CO_2/H_2 selectivity changed only slightly. Zheng et al. [6] prepared Pebax 1657 MMM with different ZIF-8 sizes of 40, 60, 90, and 110 nm. 5 wt.% loading of 90-nm ZIF-8 resulted in CO_2 permeability of 99.7 Barrer and CO_2/N_2 selectivity of 59.6, which was improved by 25% compared to pure Pebax.

The size of inorganic filler ZIF-8 has been modified to enhance interface compatibility between polymer and inorganic particles [7]. Zheng et al. [6] and Jomekian et al. [7] synthesized ZIF-8 particles on Pebax 1657 by controlling molar ratio of precursors of ZIF-8 to enhance CO_2 permeability and selectivity of CO_2/N_2. Nafisi et al. [3] filled ZIF-8 particles into Pebax 2533 to compare with pure Pebax 2533 to enhance CO_2 permeability. However, research on Pebax 2533/ZIF-8 MMMs has not been studied enough, and the characteristic of Pebax 2533 when the sizing technique of ZIF-8 nanoparticles is applied to enhance CO_2 permeability has not been investigated yet. In this study, ZIF-8 synthesized with three different molar ratios of precursors was introduced both into Pebax 1657 and Pebax 2533. The impact of controlling molar ratio of ZIF-8 precursors on structural change of Pebax1657/ZIF-8 MMMs and Pebax 2533/ZIF-8 MMMs were investigated to confirm the highest CO_2 permeability and CO_2/N_2 ideal selectivity. The permeability and selectivity results are explained in terms of the chemical structure of Pebax, and the morphological changes and crystallinity of ZIF-8 were analyzed by SEM and XRD. Pebax 2533 (80% of PTMEO and 20% of PA12) shows higher permeability than Pebax 1657 (60% of PEO and 40% of PA6) because it has higher content of PE, which is highly associated with gas transport, and it also has PTMEO, instead of PEO, which has higher diffusivity [24]. However, Pebax 1657 shows higher CO_2/N_2 selectivity than Pebax 2533 because PEO segment in Pebax 1657 has higher affinity to CO_2 than PTEMO segment in Pebax 2533. PA content in Pebax corresponds to the crystallinity region in polymeric matrix in Pebax, which directly contributes to a decrease of permeability as PA loading increases [24]. Therefore, Pebax 2533 is known to be the most efficient copolymer for CO_2 permeation, and Pebax 1657 has been widely used for MMMs with ZIF-8, which is why they were chosen to find the optimal conditions for Pebax/ZIF-8 MMMs.

2. Materials and methods

2.1. Synthesis of ZIF-8 particles

ZIF-8 nanoparticles were synthesized with different molar ratios of the precursors 2-methylimidazole (99%, 2-MeIM) and zinc nitrate hexahydrate (99%, $Zn(NO_3)_2{\cdot}6H_2O$) (Merck, Inc.). The molar ratios of 2-MeIM/$Zn(NO_3)_2{\cdot}6H_2O$ (2-MeIM/Zn) were set as 2/1, 8/1, and 32/1 [7,25]. Furthermore, 0.55 g, 2.2 g, and 8.8 g of 2-MeIM were used with 1 g of $Zn(NO_3)_2{\cdot}6H_2O$ to obtain molar ratios of ZIF-8 particles of 2/1, 8/1, and 32/1, respectively. Each precursor was dissolved in 200 ml of methanol (99.99%, MeOH) separately. A cloudy solution was obtained after vigorous stirring for 1 h. The obtained solution was centrifuged for 1 h at 5,000 rpm to separate the synthesized ZIF-8 particles from the methanol solution. The deposited ZIF-8 powder was prepared by pouring methanol solution and drying at ambient temperature for 24 h [7,25].

2.2. Preparation of Pebax/ZIF-8 MMMs

Pebax 1657 and Pebax 2533 were provided by Arkema, Inc. Pebax 1657 and Pebax 2533 were dissolved at 3 wt.% in a solution of ethanol (99.99%, EtOH)/deionized water (70 wt.%/30 wt.%) at 75˚C for 2 h [6] and in 1-butanol (99.99% BuOH) at 80˚C for 3 h [3], respectively. Next, 10 wt.% of each of the three different ZIF-8 powders molar ratios 2/1, 8/1, and 32/1 were added based on the ZIF-8 loading equation (Eq. (1)). Selected loading of ZIF-8 was based on the most common range of ZIF-8 loading, which are between 2 wt.% to 20 wt.%. As ZIF-8 loading increases the CO_2 permeability tends to increase, whereas the CO_2/N_2 selectivity decreases. Zheng et al. reported that as ZIF-8 loading increased from 5 wt.% to 20 wt.%, CO_2 permeability of ZIF-8/Pebax MMMs loading was increased from 99.7 to 156.2 Barrer, whereas CO_2/N_2 selectivity was decreased from 59.6 to 40.5. ZIF-8 powder was dispersed in the prepared solutions by an ultrasonication bath for 10 min. The prepared solutions of Pebax/ZIF-8 MMMs were poured in Teflon dishes and dried in a vacuum oven at 50˚C for 72 h.

$$\textit{ZIF-8 loading (wt. \%)} = \frac{m_{ZIF-8}}{m_{Pebax}+m_{ZIF-8}} \times 100\ \% \quad (1)$$

Table 1 shows the abbreviations of synthesized Pebax/ZIF-8 MMMs with different 2-MeIM/Zn of 10 wt.% of ZIF-8.

2.3. Permeability test

Gas permeation tests with a single gas (CO_2 or N_2) were performed using a flat sheet module at constant volume. The single gas tests were performed at a feed pressure of 4 bar and increasing temperatures of 15, 35, 55, and 75˚C. The CO_2 and N_2 permeabilities were calculated with the various temperatures of the feed gas while maintaining differences of pressure between the feed side and permeate side based on the following equation:

$$P = \frac{VL}{ART\,(p_{feed}-p_{permeate})}\left(\frac{dp_{permeate}}{dt}\right) \quad (2)$$

where P is the permeability of CO_2 and N_2 (Barrer, 1 Barrer = 10^{-10} cm^3 (STP) cm cm^{-2} s^{-1} $cmHg^{-1}$), V is the volume of the permeate side of the membrane (cm^3), L is the thickness of the membrane (cm), p_{feed} is the pressure of the feed, $p_{permeate}$ is the pressure of the permeate (cmHg s^{-1}), T is the varied temperature of the feed side (K), A is the membrane area (cm^2), $\frac{dp_{permeate}}{dt}$ is the rate of pressure of the permeate side (cmH s^{-1}), and R is the ideal gas

constant (0.278 cmHg cm^3 cm^{-3} (STP) K^{-1}).

The permeation ideal selectivity of CO_2 and N_2 was calculated using the permeability ratio of the more permeable gas (CO_2) to the less permeable gas (N_2).

$$\alpha_{CO_2/N_2} = \frac{P_{CO_2}}{P_{N_2}} \quad (3)$$

2.4. Characterization

FE-SEM (JSM-7800F Prime, JEOL Ltd, Japan) at 10-15 kV was used to characterize the size and morphology of the ZIF-8 nanoparticles and to obtain surface and cross-sectional images of Pebax 1657/ZIF-8 MMM and Pebax 2533/ZIF-8 MMM. Powder X-ray diffraction (XRD) (SmartLab, Rigaku, Japan) was performed on the ZIF-8 nanoparticles, pure Pebax, and Pebax/ZIF-8 MMM to determine the crystallinity. XRD was applied with Cu Ka radiation (40 kV-40mA) at a scan speed of 2˚/min and step size of 0.02˚ by scanning 2θ angles between 5˚ and 60˚. A differential scanning calorimeter (DSC) (Discovery DSC, TA Instrument, USA) was used to determine the thermal properties of pure Pebax and Pebax/ZIF-8 MMM at a temperature range of -70 to 230˚C at a scanning rate of 10˚C /min.

Table 1
The abbreviated names of all Pebax/ZIF-8 MMMs with different 2-MeIM/Zn of 10 wt.% of ZIF-8.

Full name of Pebax/ZIF-8 MMM	Abbreviated name of MMM
Pebax 1657/ZIF-8 2/1M	P1/Z2
Pebax 1657/ZIF-8 8/1M	P1/Z8
Pebax 1657/ZIF-8 32/1M	P1/Z32
Pebax 2533/ZIF-8 2/1M	P2/Z2
Pebax 2533/ZIF-8 8/1M	P2/Z8
Pebax 2533/ZIF-8 32/1M	P2/Z32

3. Results and discussion

3.1. Characterization of ZIF-8

The SEM images (Figure A1, see appendix) of ZIF-8 were analyzed to compare the sizes and shapes obtained with increasing molar ratios of 2-MeIM/Zn. As the molar ratio of 2-MeIM/Zn increased, the size of ZIF-8 particles decreased, which are in good agreement with the results reported by Jomekian et al. [7,25]. Size distributions of Z2, Z8, and Z32 ranged from 295.3 nm to 712.4 nm, 220.2 nm to 531.2 nm, and 105.7 nm to 458.7 nm, respectively. The average size of Z2, Z8, and Z32 were 500.7, 363.3, and 217.1 nm, respectively.

The increase in concentration of 2-MeIM generates the large number of nuclei, which decreases the actual crystal size of ZIF-8 particle [26]. As 2-MeIM/Zn molar ratio increased, ZIF-8 particles changed from cubical to spherical shape [6] and particle aggregation was formed.

The X-ray diffraction was used to characterize the crystallinity of the ZIF-8 structures (Figure 1). As molar ratios of 2-MeIM/Zn increased, the intensity of characteristic XRD peaks decreased, and the peak became wider [6]. The decrease of XRD peaks with increasing 2-MeIM/Zn resulted from excess of MeIM [27]. The excess MeIM on the particle surface prevented particle growth, resulting in decrease of crystallinity [27]. Furthermore, the XRD pattern obtained with decreasing molar ratio of 2-MeIM/Zn showed higher and narrower peaks [6]. This means that the ZIF-8 is crystalline with decreasing 2-MeIM/Zn and is amorphous with increasing 2-MeIM/Zn [12]. This can be characterized by the Scherrer equation, in which the peak width is inversely proportional to the crystal size:

$$B(2\theta) = \frac{K\lambda}{L\cos\theta} \quad (4)$$

where B is the peak width, K is proportionality constant called the Scherrer constant, θ is the Bragg angle, and L is the crystallite size.

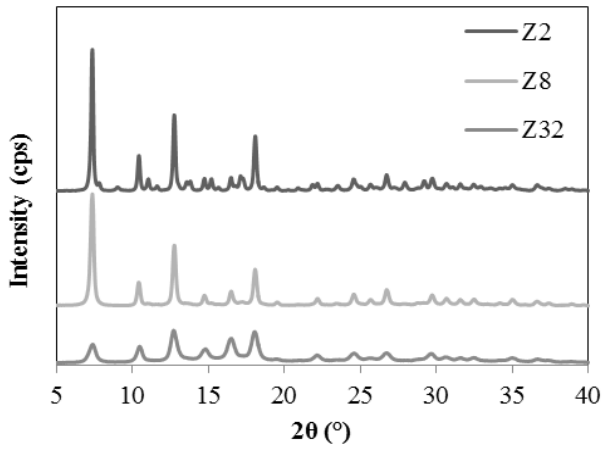

Fig. 1 XRD graphs of ZIF-8 particles with different molar ratio of 2-MeIM/Zn.

3.2. Characterization of Pebax/ZIF-8 MMMs

The XRD patterns of Pebax 1657/ZIF-8 MMMs and Pebax 2533/ZIF-8 MMMs show the crystallinity of both Pebax and ZIF-8 (Figures 2 and 3). In Figure 2, P1 shows a broad peak in the range of 16.8 to 22.7˚ and a sharp peak at 24˚, which represents the amorphous PEO segment and crystalline PA segment, respectively [12,28]. Distinct peaks of ZIF-8 in MMMs at 7.3˚, 10.4˚, 14.7˚, and 26.7˚were observed in the XRD pattern of Pebax 1657/ZIF-8, which are in good agreement with other studies [12,13,29]. From the peak range of the PEO segment (between 16.8˚ and 22.7˚), P1/Z32 showed the most similar pattern to P1, as Z32 has more amorphous structure than Z8 or Z2 (Figure 1). From the peak of the PA segment at 24˚, P1/Z2 showed more obvious and distinct PA peaks than P1/Z8 and P1/Z32 because Z2 has more crystalline structure than Z8 or Z32 (Figure 1). As molar ratio of ZIF-8 precursors increases, the crystal growth decreases as concentration of unreacted 2-MeIM increases; whereas concentration of Zn stays constant, resulting in less crystalline structure [27].

In Figure 3, P2 showed a peak at 20˚ for the crystalline PA segment, which agrees with previous work by Kim et al. [30]. Distinct peaks of ZIF-8 at 7.3˚, 10.4˚, and 14.7˚ were also observed in the pattern of Pebax 2533/ZIF-8 XRD pattern. P2/Z2 showed the highest peak compared to P2/Z8 and P2/Z32, as in the XRD patterns of Pebax 1657/ZIF-8 MMM.

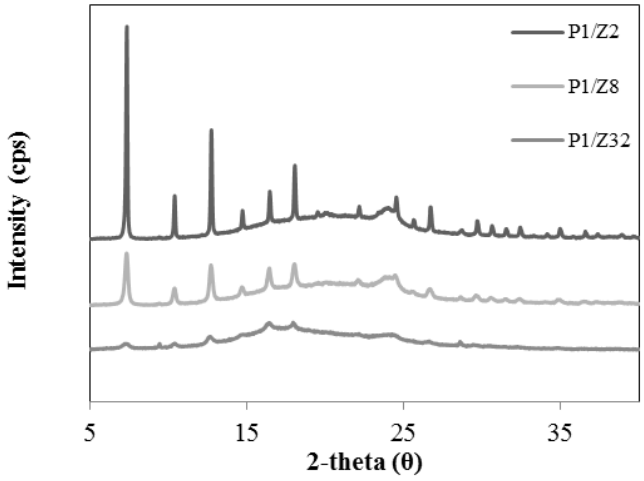

Fig. 2. XRD graphs of P1, P1/Z2, P1/Z8, and P1/Z32.

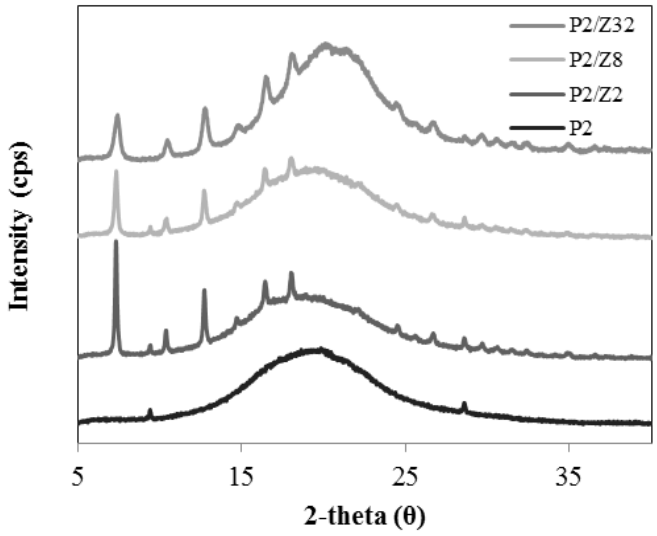

Fig. 3 XRD graphs of P2, P2/Z2, P2/Z8, and P2/Z32.

The DSC curves (Figures A2-A9, see appendix) were analyzed to determine the glass transition temperatures of PE and PA in the Pebax and Pebax/ZIF-8 MMMs. The polymer crystallinity can be determined by measuring the enthalpy of fusion of the polymer [12,31] (Eq. (5)).

$$X_c = \frac{\Delta H_m}{\Delta H^\circ_m} \quad (5)$$

where ΔH_m is the melting enthalpy of a semi-crystalline polymer and ΔH°_m is the melting enthalpy of the pure crystalline of PE and PA. The melting enthalpy of PEO, PTMEO, and PA were 166.4 J/g, 200 J/g, and 230 J/g, respectively, which were obtained from literature [12,31,32]. The membrane crystallinities of PE and PA segments of Pebax/ZIF-8 MMMs were calculated (Table 2). The crystallinity in Pebax 1657 MMMs was lowest in P1/Z32. On the other hand, the crystallinity in Pebax 2533 MMMs was lowest in P2/Z2. Both DSC results of Pebax/ZIF-8 MMMs were in good agreement with XRD results.

Table 2
The degree of crystallinity of Pebax and Pebax/ZIF-8 MMMs based on DSC results.

	ΔH_m (PE) (J/g)	ΔH_m (PA) (J/g)	X_{PE} (%)	X_{PA} (%)	Xc
P1	17.70	17.69	10.64	7.70	9.5
P1/Z2	17.35	17.38	10.43	7.56	9.3
P1/Z8	16.80	16.71	10.09	7.27	9.0
P1/Z32	13.09	17.19	7.87	7.47	7.7
P2	31.37	4.51	15.68	1.96	12.9
P2/Z2	27.48	5.48	13.74	2.38	11.5
P2/Z8	28.73	5.24	14.36	2.28	11.9
P2/Z32	29.94	6.58	14.97	2.86	12.5

3.3. The effect of controlling molar ratio of ZIF-8 on gas permeability of Pebax/ZIF-8 MMMs

Figures 4 and 5 showed that the CO_2 permeability of Pebax 2533 MMMs was much higher than that of Pebax 1657 MMMs at the same temperature. The different CO_2 permeabilities can be explained by the chemical structure and affinity with CO_2 gas molecules. The effect of increasing molar ratios of 2-MeIM/Zn on the CO_2 permeability of Pebax/ZIF-8 MMMs (Figures 4 and 5) was investigated. At a temperature of 15˚C, Pebax 1657/ZIF-8 MMM showed the highest CO_2 permeability with P1/Z32, followed by P1/Z8 and P1/Z2. At the same temperature, Pebax 2533/ZIF-8 MMM showed the highest CO_2 permeability for P2/Z2, followed by P2/Z8 and P2/Z32.

Bondar et al. [24] and Kim et al. [30] explained the difference in permeability of the two types of Pebax in terms of chemical structure, diffusivity, polarity, and solubility of Pebax. The chemical structure of Pebax 2533 has a higher content of rubbery PTMEO, which is a gas-transport-dominating phase, so it has higher permeability than Pebax 1657 [24]. The diffusivity of Pebax 1657 is lower than that of Pebax 2533 because it has more concentrations of polar groups in polymer matrix, which lowers gas diffusion coefficient [24]. However, the CO_2/N_2 selectivity of Pebax 1657 may be higher than that of Pebax 2533 because the diffusivity of Pebax 1657 is lower for nonpolar gases, such as N_2, and the solubility is higher for polarizable gases like CO_2 [30,33].

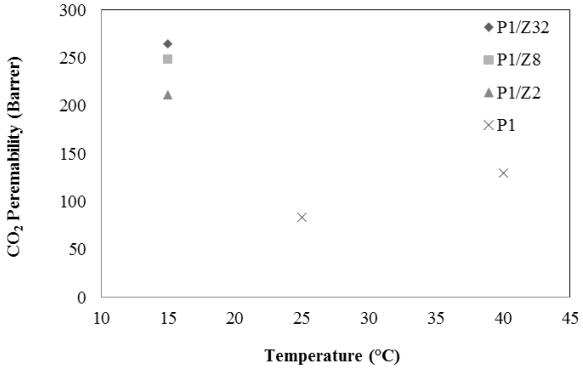

Fig. 4. CO_2 permeability of P1, P1/Z2, P1/Z8, and P1/Z32.

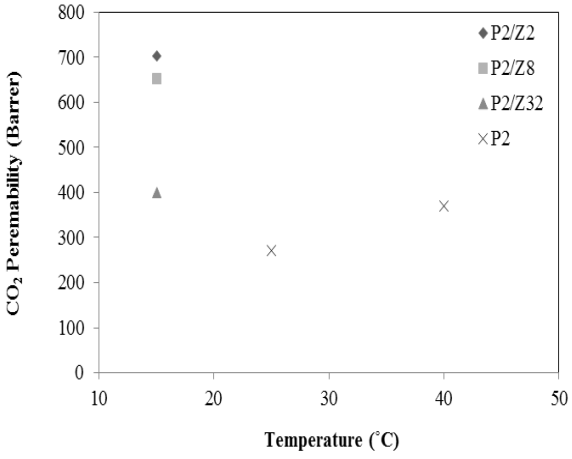

Fig. 5. CO_2 permeability of P2, P2/Z2, P2/Z8, and P2/Z32.

There are several important factors in the opposite trends of CO_2 permeability for Pebax 1657/ZIF-8 and Pebax 2533/ZIF-8 based on different molar ratios of ZIF-8 precursors (Figures 4 and 5): (1) particle size, numbers of pore, and pore size of ZIF-8 with increasing molar ratio of 2-MeIM/Zn, (2) the polarity of Pebax, (3) the affinity for CO_2 gas molecules, and (4) the crystallinity change of Pebax MMMs in terms of ZIF-8 molar ratio.

For Pebax 1657 MMMs, as the molar ratio 2-MeIM/Zn of ZIF-8 precursors increased, the CO_2 permeability at a fixed temperature of 15°C increased (Figure 4). Jomekian et al. [7] reported on the trend of increasing permeability of Pebax 1657/ZIF-8 corresponding to increasing molar ratios of 2-MeIM/Zn. The increasing molar ratio of 2-MeIM/Zn increases the CO_2 permeability by higher gas sorption capacity [7]. Increasing the molar ratio of 2-MeIM/Zn showed higher numbers of nanopores, which are related to high sorption capacity [7]. As the sizes of nanoparticles decrease, the surface areas become larger and create interfacial regions in the organic polymers.

Furthermore, the gas adsorption is enhanced as the numbers of pores in ZIF-8 particles are increased [7,33].

The polarity of Pebax is another important factor of the permeability increase of Pebax 1657 MMMs with increasing molar ratio 2-MeIM/Zn of ZIF-8. Pebax 1657 has a high concentration of polar groups in PEO chain segments, which have a high affinity for CO_2 [24]. Imidazolium ions and PEO segments in the Pebax 1657 result in excessive adsorption of CO_2 molecules [7]. Excessive sorption of CO_2 by imidazolium ions causes plasticization of Pebax 1657, which enhances the polymer chain mobility [7, 34]. The result of highest permeability of Pebax 1657 with increasing 2-MeIM/Zn can be also explained by the crystallinity change with incorporation of ZIF-8 with increasing 2-MeIM/Zn. As described in subsection 3.2, P1/Z32 showed the lowest crystallinity in DSC results (Table 2), which also showed the highest CO_2 permeability.

However, for Pebax 2533 MMMs, increasing the molar ratio of ZIF-8 resulted in lower CO_2 permeability at 15˚C (Figure 5). When the molar ratio of 2-MeIM/Zn increases, the shape of ZIF-8 particles changes from cubical to spherical (Figure 1A), and as a result, the fillers aggregate and tend to fill the interstitial regions of the polymer, which could prevent access to the polymer matrix [35]. The diffusivity may be decreased by the smaller pore size and particle size of ZIF-8 with increasing molar ratio of 2-MeIM/Zn. According to Jomekian et al. [7,25], increasing the ZIF-8 molar ratio decreases the particle size and pore volume of ZIF-8 particles. As molar ratio of ZIF-8 increases, the particle size of ZIF-8 decreases along with the pore size [7,25]. This implies that particles aggregate more and may reduce space in the polymer matrix for penetrants to diffuse.

Compared to Pebax 1657, the polarity of Pebax 2533 is lower in the PTMEO segment, which has a low affinity for CO_2 [24]. When the molar ratio of 2-MeIM/Zn increases, the concentration of polar imidazolium ions in ZIF-8 increases. However, less polar PTMEO in Pebax 2533 may not be enough to interact with imidazolium to adsorb CO_2 and enhance the polymer chain mobility. It suggests that increasing the molar ratio of ZIF-8 can prevent the interstitial volume from accessing the polymer segment and decrease the free volume and diffusivity. Although the loading ZIF-8 of any molar ratio in Pebax 2533 enhanced the permeability of CO_2 molecules compared to pure Pebax 2533, increasing the molar ratio was not effective for Pebax 2533 to enhance the CO_2 permeability. The result of highest CO_2 permeability of Pebax 2533 with decreasing 2-MeIM/Zn can be also explained by the lowest crystallinity of P2/Z2 in DSC results (Table 2).

The incorporation of ZIF-8 in Pebax MMMs enhanced the CO_2 permeability for both Pebax 1657 and 2533 by increasing CO_2 diffusivity and solubility. The hydrogen bonds between ZIF-8 and PA segment stabilized the structure of MMMs and disrupted PEO segment, which enhanced free volume, decreased the crystallinity of PEO, and increased the CO_2 permeability of Pebax MMMs. Pebax 1657 MMM showed highest CO_2 permeability with increasing molar ratio of ZIF-8, which agrees with the lowest crystallinity of P1/Z32 in the DSC results. Pebax 2533 MMM showed highest CO_2 permeability with decreasing molar ratio of ZIF-8, which agrees with the lowest crystallinity of P2/Z2 in the DSC results. Therefore, Pebax 1657 was more effective for the permeation of CO_2 with Z32, whereas Pebax 2533 was more effective for the permeation of CO_2 with Z2. The ZIF-8 filler increased the CO_2 solubility of Pebax 1657 more than that of Pebax 2533 through CO_2 sorption of the polar groups in organic ligand of 2-MeIM [12].

Even though the permeation tests for pure Pebax and Pebax/ZIF-8 MMMs were performed at different temperatures due to the limitation related to experimental set up, the permeability of pure Pebax 1657 was 83.7 Barrer at 25˚C and 130 Barrer at 40˚C, whereas the lowest permeability of P1/Z2 was 212 Barrer at 15˚C (Figure 4). The permeability of pure Pebax 2533 was 272 Barrer at 25˚C and 370 Barrer at 40˚C, whereas the lowest permeability of P2/Z32 was 399 Barrer at 15˚C (Figure 5). Therefore, the CO_2 permeability of Pebax/ZIF-8 MMM was higher than those of both Pebax 1657 and Pebax 2533 alone, even at lower temperature.

The higher CO_2 permeability of Pebax with the incorporation of ZIF-8 particles can be achieved by high CO_2 solubility and diffusivity of ZIF-8 [1,12]. CO_2 adsorption capacity in ZIF-8 is high because polar organic ligands of 2-MeIM in ZIF-8 adsorb polarizable CO_2 molecule selectively, which can improve CO_2 solubility [1,7,12]. Flexible porous structures of ZIF-8 increase free volume in Pebax matrix, which can improve diffusion of gas molecules with large kinetic diameters [13].

The enhancement of the free volume is a mechanism for increasing diffusion, which is described by the Cohen and Turnbull equation (Eq. (6)) [36]:

$$D = A\ exp\left(\frac{-\gamma V^*}{V_f}\right) \quad (6)$$

where D is the diffusion coefficient, A is the pre-exponential factor, γ is an overlap factor to avoid the double-counting of free volume elements, V^* is the minimum free volume element size that a penetrant can pass, and V_f is the average free volume in the polymer that is available for a penetrant to be transported through [37]. Therefore, incorporation of ZIF-8 on Pebax increases both diffusivity and solubility, which can improve the permeability based on the solution-diffusion mechanism in Eq. (7):

$$P_i = D_i * S_i \quad (7)$$

where P_i is the permeability of gas i, D_i is the average effective diffusion coefficient, and S_i is the solubility coefficient.

Furthermore, at the interfacial region between ZIF-8 and Pebax, ZIF-8 particles form hydrogen bonding with PA in Pebax, which occur between (1) the aldehyde groups in the PA segment and methyl groups in the 2-methylimidazole in the ZIF-8, as well as (2) N-H groups in the PA and N atoms of the imidazole ring [19,20]. ZIF-8 particles not only enhance structural stability by forming hydrogen bonds with PA [12], but also disrupt chain packing of PEO segment in Pebax [12]. As the chain packing is disrupted, the PEO chain interaction is decreased, resulting in increasing free volume for penetrants to diffuse [12]. Also, the disrupted PEO chain packing results in decrease of the crystallinity of PEO segment [35]. Kim et al. [30] reported that the crystallinity region in a Pebax polymeric matrix decreases the permeability of the Pebax because the crystalline phase forms uniform and rigid chains that lack sorption sites and the mobility of chains for the permeation of penetrants.

3.4. The effect of temperature on gas permeability of Pebax/ZIF-8 MMMs with different molar ratio of ZIF-8

To confirm the effect of the permeating temperature on Pebax MMMs, the MMMs with the highest permeabilities were tested with CO_2 gas and N_2 gas at increasing temperature. Pebax 1657/ZIF-8 MMM with a molar ratio of 32/1 and Pebax 2533/ZIF-8 with molar ratio of 2/1 were used at a constant feed pressure of 4 bar and temperatures of 15, 35, 55, and 75˚C. As the temperature increased, the CO_2 permeability obtained with both P1/Z32 and P2/Z2 increased.

The temperature dependency of the permeability was calculated using the van't Hoff-Arrhenius equation (Eq. (8)):

$$P = P_o\ exp\left(-\frac{E_P}{RT}\right),\ E_p = E_d + \Delta H_s \quad (8)$$

where P is the permeability coefficient, P_0 is a pre-exponential factor, and E_P is the activation energy of permeation, which is the sum of the activation energy for diffusion, E_d, and the enthalpy of sorption, ΔH_s [30,37]. R is the gas constant, and T is the operating temperature [38]. Based on this equation, if either the activation energy for diffusion or the enthalpy of sorption decreases, the permeability increases.

A logarithmic function was applied to the van't Hoff-Arrhenius equation (Eq. (9)) to calculate the pre-exponential factor P_o and activation energy of permeation, E_p (Figures 6 and 7):

$$log\ P = -\frac{E_p}{R}\cdot\frac{1}{T} + log\ P_o \quad (9)$$

The activation energy of permeation can be calculated from the slope of the log of permeability, $-\frac{E_p}{R}$. Before filling the Pebax polymer with ZIF-8, the activation energy of permeation of Pebax 2533 (16.7 kJ/mol) is lower than that of Pebax 1657 (18.6 kJ/mol) (Table 3) [39].

However, from the calculation of P_o and E_p of P1/Z32 and P2/Z2 (Table 3), the activation energy of diffusion of P1/Z32 (5.2 kJ/mol) is lower than that of P2/Z2 (9.7 kJ/mol). The polar PEO chains of Pebax 1657 interact with highly polar imidazolium ions in ZIF-8 nanoparticles and both of them have high affinity for CO_2. Therefore, CO_2 molecules are excessively adsorbed, which results in plasticization [7,12,40]. This decreases the enthalpy of sorption, resulting in lower activation energy of permeation [30].

From eq. (9), the pre-exponential factor P_o can be calculated by 10 to the power of the y-intercept. The pre-exponential factor and activation energy of permeation are high when penetrants are not significantly affected by the temperature change [41]. According to Table 3, both the activation energy of permeation and pre-exponential factor of Pebax 1657 were lower than those of Pebax 2533, which means that Pebax 1657 MMM is more sensitive to temperature changes, and the permeability was increased more significantly

[41], even though the increase of temperature increases the permeability for both Pebax 1657 MMM and Pebax 2533 MMM. When the temperature increased, the interaction between more polar PEO groups in Pebax 1657 and polar imidazolium ion in ZIF-8 may have increased the permeability of penetrants. The reason is that the enthalpy of sorption is decreased by the CO_2 sorption of more polar groups in Pebax 1657 and 2-MeIM in ZIF-8 [12,30]. On the other hand, less polar PTEMO groups in Pebax 2533 are less polar to adsorb CO_2, which may result in less of a decrease in the enthalpy of sorption than that of Pebax 1657 MMM. Increasing the permeating temperature increased the permeabilities of both Pebax 1657/ZIF-8 and Pebax 2533/ZIF-8. However, the permeability of Pebax 1657/ZIF-8 MMM was more dependent on the temperature, which was proven by the low activation energy of permeation.

As the permeating temperature increased, the ideal selectivity of CO_2/N_2 decreased for both P1/Z32 and P2/Z2 (Figures 8 and 9). This phenomenon occurred for both Pebax/ZIF-8 and pure Pebax. Kim et al. [30] reported that the CO_2/N_2 selectivity of Pebax 1657 decreased. As the temperature increases, the polymer loses its chemical nature of favoring particular gases because segmental motion of the gas molecules increases regardless of the penetrants [41]. Also, the flexible structure of ZIF-8 in Pebax MMMs creates a pore that increases micro-void for diffusion of all gas molecules [12,13].

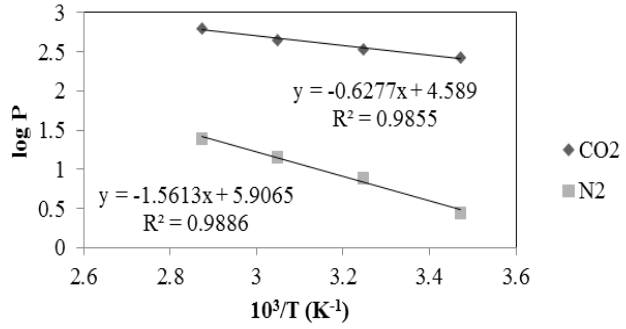

Fig. 6. The correlation of permeability and temperature with preexponential constant (P_o) and activation energy of permeation (E_p) of P1/Z32.

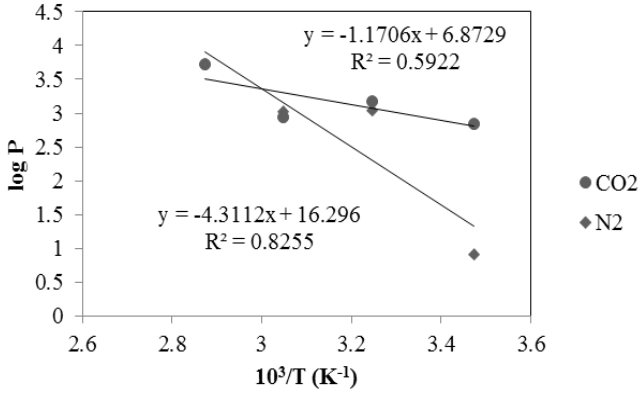

Fig. 7. The correlation of permeability and temperature with preexponential constant (P_o) and activation energy of permeation (E_p) of P2/Z2.

Furthermore, Bondar et al. [24] explained that the selectivity of polarizable CO_2/nonpolar gases like N_2 is lower for PTMEO/PA12 copolymers because they have less polar ether linkages to adsorb CO_2 than PEO/PA6 copolymers. Pebax 2533 has a higher concentration of PTMEO (a transport-dominating phase) than the concentration of PEO in Pebax 1657, which enhances the diffusivity. Therefore, based on Figures 8 and 9, Pebax 1657 was more suitable for increasing the CO_2/N_2 ideal selectivity through interactions with polar imidazolium ions at a molar ratio 32/1 of ZIF-8. On the other hand, Pebax 2533 was more suitable for increasing the CO_2 permeability through increasing the fractional free volume of the polymeric matrix by adding less aggregating ZIF-8 with a molar ratio of 2/1.

Table 3
Activation energy of permeation (E_p) and pre-exponential factor (P_o) of P1/Z32 and P2/Z2 compared to pure Pebax membranes.

MMMs	Penetrant Gas	E_p (kJ/mol)	P_o (Barrer)	Ref.
P1/Z32	CO_2	5.2	3.88×10^4	This work
	N_2	13	8.06×10^5	This work
Pebax 1657	CO_2	18.6		[39]
P2/Z2	CO_2	9.7	7.46×10^6	This work
	N_2	35.8	1.98×10^{16}	This work
Pebax 2533	CO_2	16.7		[39]

The performance of Pebax 1657/ZIF-8 MMMs and Pebax 2533/ZIF-8 MMMs synthesized with three different types of ZIF-8 at 35˚C is presented with Robeson upper bound line on Figure 10. Based on Robeson graph [11], P1/Z32 at temperature 35˚C showed the most ideal performance satisfying both high CO_2 permeability and CO_2/N_2 ideal selectivity. P2/Z2 showed higher CO_2 permeability compared to P1/Z32 at 35˚C, but CO_2/N_2 ideal selectivity values are far beneath the Robeson upper bound. As observed in Figures 8 and 9, Pebax/ZIF-8 MMMs showed that as temperature increases, the CO_2 permeability increases but the ideal selectivity is decreased. The result of Pebax 2533/ZIF-8 MMMs are far beneath the Robeson upper bound, which indicating very low CO_2/N_2 ideal selectivities.

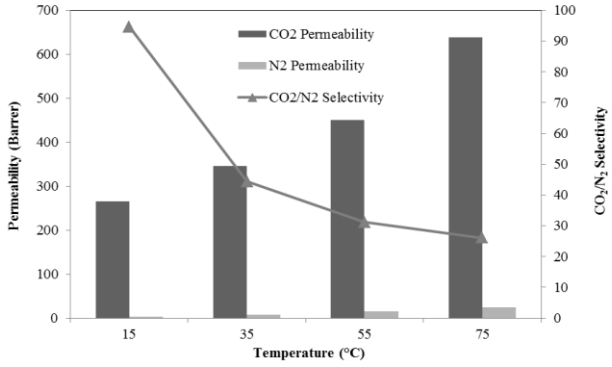

Fig. 8. Single CO_2 and N_2 gas permeability and CO_2/N_2 ideal selectivity of P1/Z32 with increasing temperature.

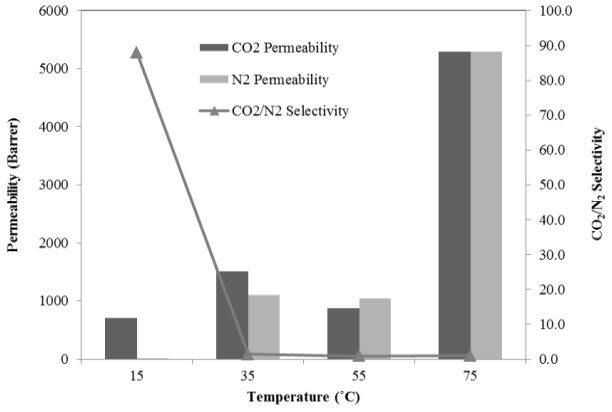

Fig. 9. Single CO_2 and N_2 gas permeability and CO_2/N_2 ideal selectivity of P2/Z2 with increasing temperature.

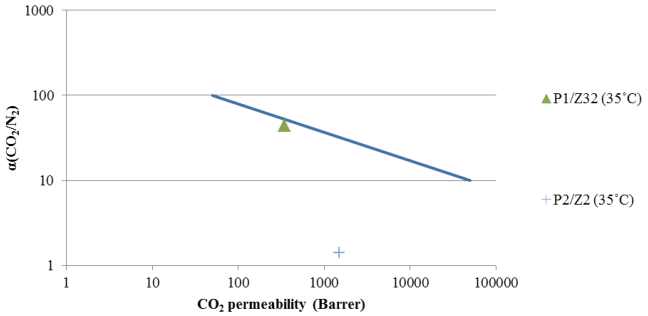

Fig. 10 Comparison between Robeson upper bound (straight line) and this work (symbols).

4. Conclusions

In this study, the effect of molar ratio of ZIF-8 precursors on the performance of CO_2 and N_2 permeation of Pebax 1657 and Pebax 2533 MMMs was investigated. Studies of CO_2 permeability of Pebax 1657/ZIF-8 MMMs with controlling molar ratio of ZIF-8 has been reported by previous research. However, CO_2 permeability of Pebax 2533/ZIF-8 MMMs with controlling molar ratio was investigated in this work, which was explained by the important relationship between ZIF-8 and Pebax based on their chemical structures and morphological characteristics that determine the CO_2 permeability. ZIF-8 with a higher molar ratio of 2-MeIM/Zn had a smaller size and showed weaker and wider peaks in XRD spectra than that of ZIF-8 with a lower molar ratio of ZIF-8 precursors (2-MeIM/Zn), which represents the chemical nature of an amorphous material.

The CO_2 and N_2 permeability were higher in Pebax/ZIF-8 MMMs than in pure Pebax. In terms of different molar ratio of ZIF-8, the CO_2 and N_2 permeability were highest for Pebax 1657 MMM with ZIF-8 molar ratio of 32/1 and for Pebax 2533 MMM with ZIF-8 molar ratio of 2/1. Compared to pure Pebax 2533, P2/Z2 showed increment of permeability by 158%, whereas compared to pure Pebax 1657, P1/Z32 showed increment of permeability by 216%. Because Pebax 1657 has a polar PE segment (60% of PEO), higher sorption capacity of ZIF-8 molar ratio of 32/1 enhanced CO_2 sorption, which resulted in improvement of CO_2 ideal selectivity over N_2. On the other hand, because Pebax 2533 has higher PE content (80% of PTMEO), but has a lower polarity that provides higher gas transport, fewer aggregating ZIF-8 particles with molar ratio of 2/1 enhanced free volume of Pebax 2533, which resulted in increase of CO_2 permeability.

The effect of temperature on the CO_2 and N_2 permeability was investigated as well. As the temperature increased, the permeabilities increased for both Pebax 1657/ZIF-8 and Pebax 2533/ZIF-8 MMMs. As the temperature increases, the diffusivity of polymer increased for all gas molecules, so the CO_2/N_2 ideal selectivity decreased for both Pebax 1657 and 2533. Also, the porous structure of ZIF-8 increased the micro-void in Pebax matrix, which increased the free volume for diffusion of all gas molecules.

In summary, Pebax 1657/ZIF-8 with a molar ratio of 32/1 and Pebax 2533/ZIF-8 with a molar ratio of 2/1 had the best performance for CO_2 permeation. This means that better permeability and compatibility between the polymer and particles can be achieved by controlling the molar ratio of ZIF-8 precursors and selecting the right Pebax polymer based on chemical nature and interfacial interactions.

Appendix

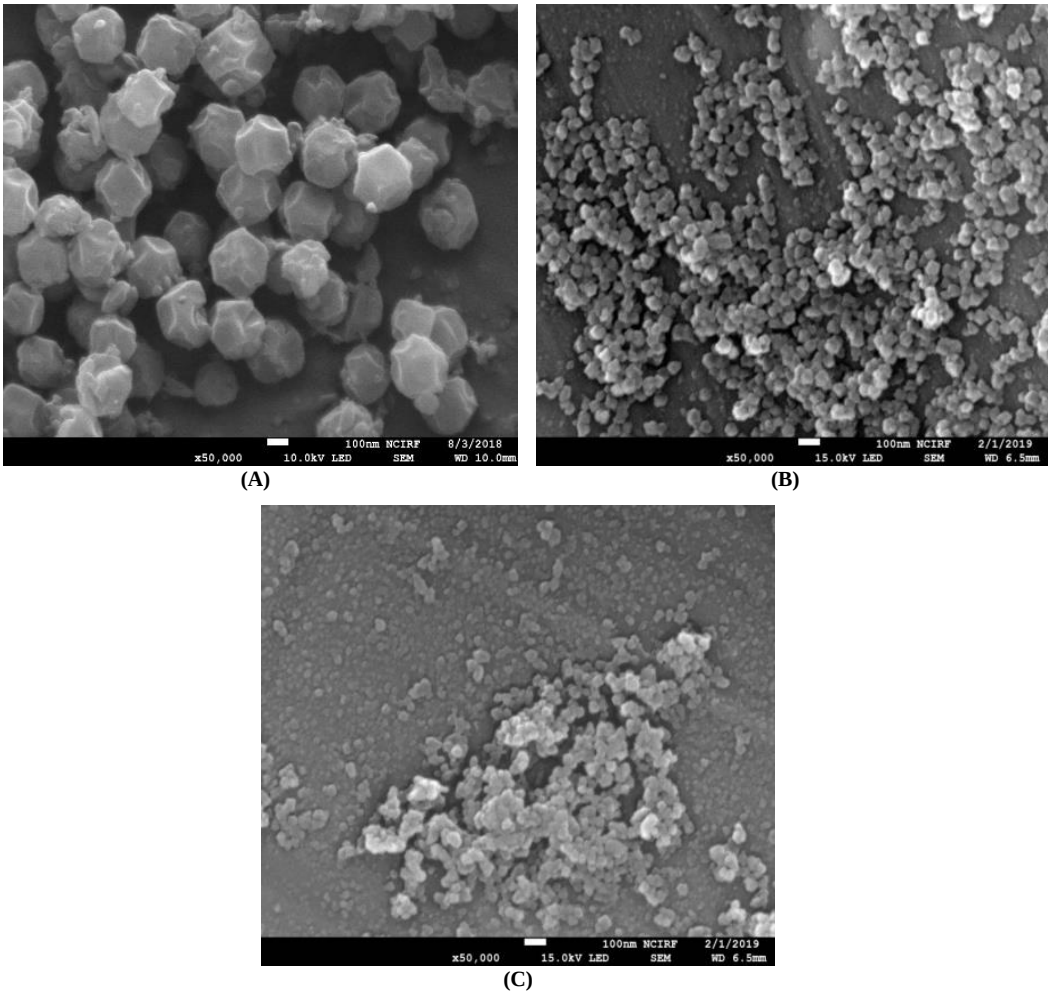

(A) **(B)**

(C)

Figure A1. SEM images of ZIF-8 particles with different 2-MeIM/Zn (A) Z2, (B) Z8, and (C) Z322.

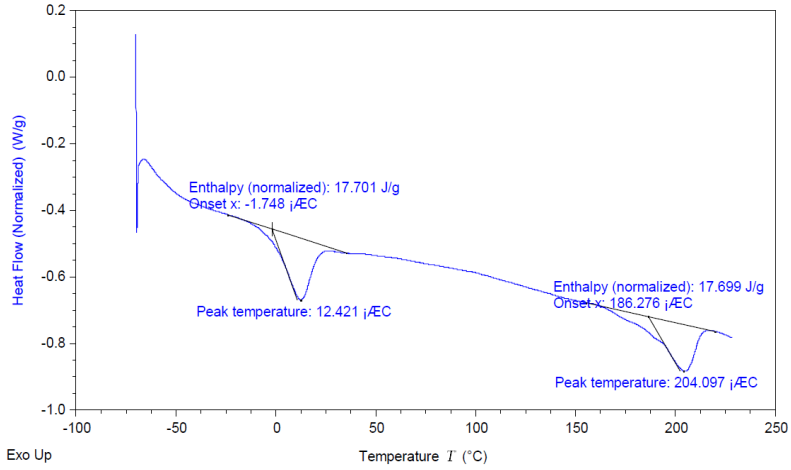

Figure A2. DSC curve of P1.

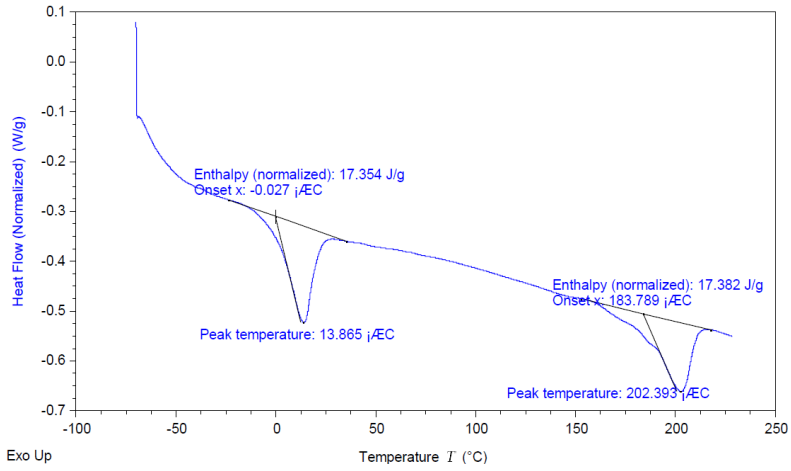

Figure A3. DSC curve of P1/Z2.

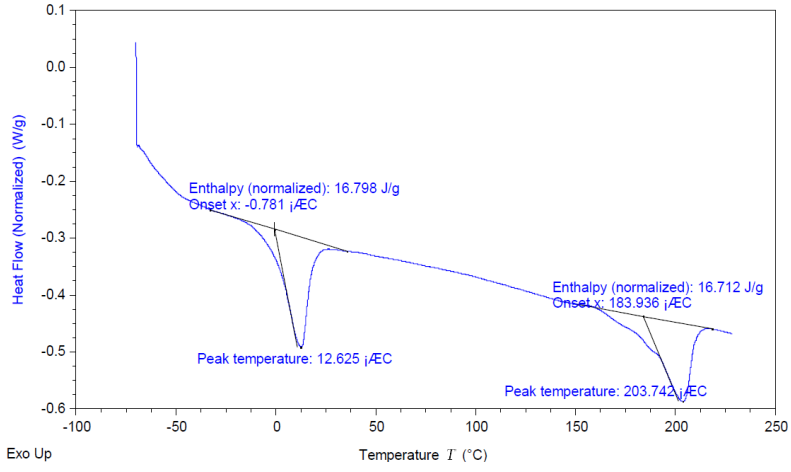

Figure A4. DSC curve of P1/Z8.

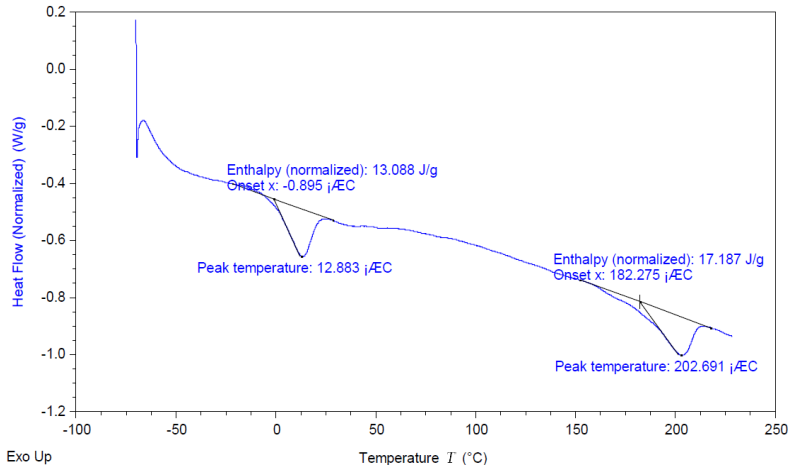

Figure A5. DSC curve of P1/Z32.

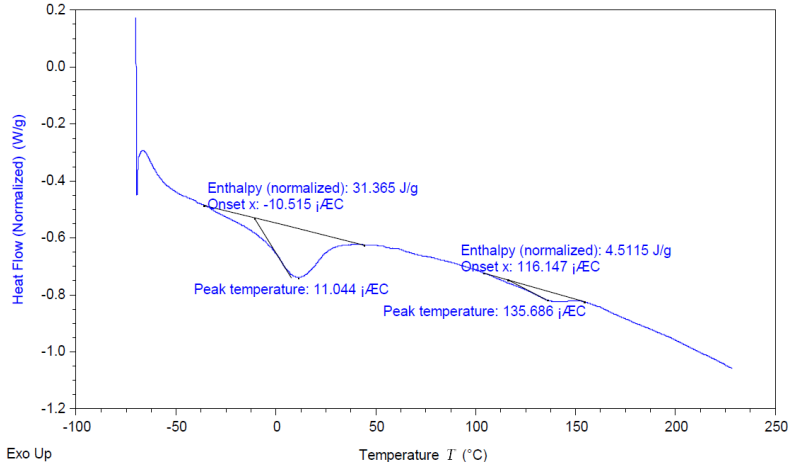

Figure A6. DSC curve of P2.

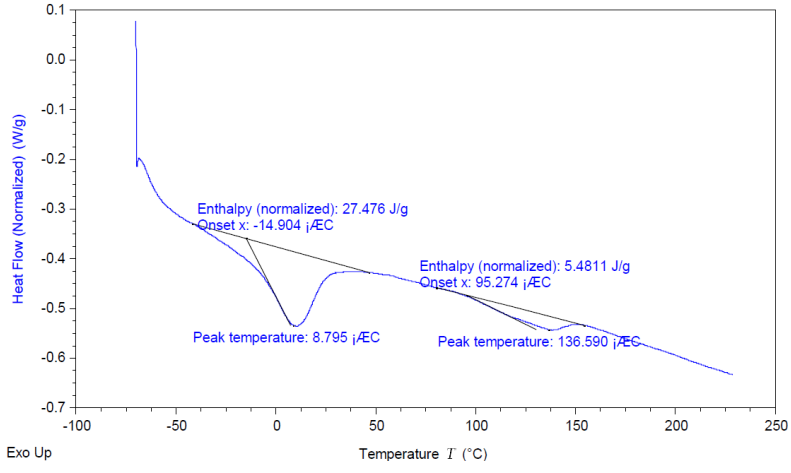

Figure A7. DSC curve of P2/Z2.

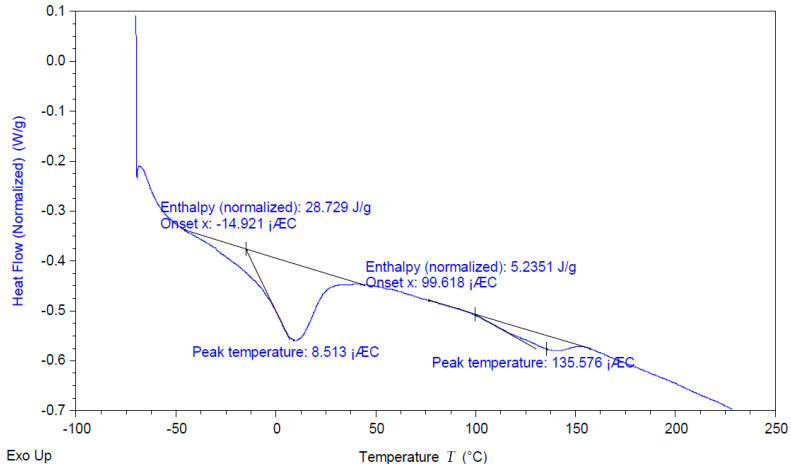

Figure A8. DSC curve of P2/Z8.

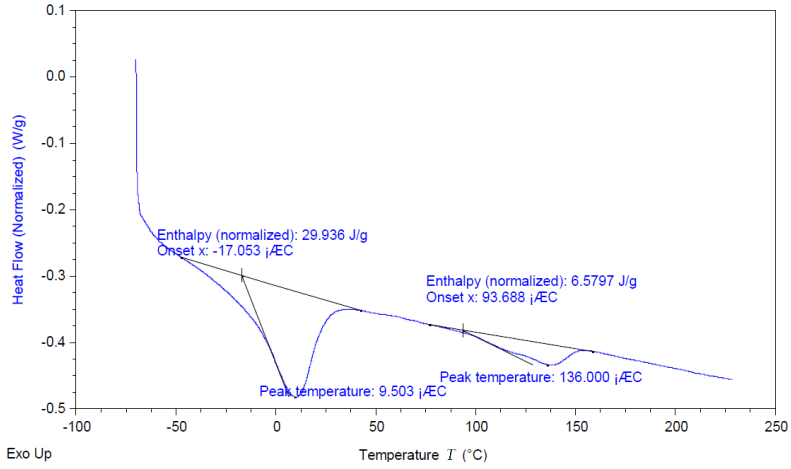

Figure A9. DSC curve of P2/Z32

Acknowledgement

This work was supported by Creative-Pioneering Researchers Program through Seoul National University (SNU).

References

[1] L. Xu, L. Xiang, C. Wang, J. Yu, L. Zhang, Y. Pan, Enhanced permeation performance of polyether-polyamide block copolymer membranes through incorporating ZIF-8 nanocrystals, Chin. J. Chem. Eng. 25 (2017) 882-891. https://doi.org/10.1016/j.cjche.2016.11.007

[2] W.J. Koros, R.P. Lively, Water and beyond: expanding the spectrum of large-scale energy efficient separation processes, AIChE J. 58 (9) (2012) 2624–2633. https://doi.org/10.1002/aic.13888

[3] V. Nafisi, M. B. Hagg, Development of dual layer of ZIF-8/PEBAX-2533 mixed matrix membrane for CO_2 capture, J. Membr. Sci. 459 (2014) 244-255. https://doi.org/10.1016/j.memsci.2014.02.002

[4] H. Lin, B.D. Freeman, Materials selection guidelines for membranes that remove CO_2 from gas mixtures, J. Mol. Struct. 739 (2005) 57-74. https://doi.org/10.1016/j.molstruc.2004.07.045

[5] K.I. Okamoto, M. Fuji, S. Okamyo, H. Suzuki, K. Tanaka, H. Kita, Gas permeation properties of poly(ether imide) segmented copolymers, Macromol. 28 (1995) 6950-6956. https://doi.org/10.1021/ma00124a035

[6] W. Zheng, R. Ding, ZIF-8 nanoparticles with tunable size for enhanced CO_2 capture of Pebax based MMMs, Sep. Purif. Technol. 214 (2018) 111-119. https://doi.org/10.1016/j.seppur.2018.04.010

[7] A. Jomekian, B. Bazooyar, R. M. Behbahni, T. Mohammadi, A. Kargari, Ionic liquid-modified Pebax 1657 membrane filled by ZIF-8 particles for separation of CO_2 from CH_4, N_2, and H_2, J. Membr. Sci. 524 (2017) 652-662. https://doi.org/10.1016/j.memsci.2016.11.065

[8] Y. Dai, X. Ruan, Z. Yan, Imidazole functionalized graphene oxide/PEBAX mixed matrix membranes for efficient CO_2 capture, Sep. Purif. Technol. 166 (2016) 171−180. https://doi.org/10.1016/j.seppur.2016.04.038

[9] R.S. Murali, A.F. Ismail, M.A. Rahman, Mixed matrix membranes of Pebax-1657 loaded with 4A zeolite for gaseous separations, Sep. Purif. Technol. 129 (129) (2014) 1−8. 10.1016/j.seppur.2014.03.017

[10] T.W. Pechar, S. Kim, B. Vaughan, E. Marand, M. Tsapatsis, H.K. Jeong, C.J. Cornelius, Fabrication and characterization of polyimide–zeolite L mixed matrix membranes for gas separations, J. Membr. Sci. 277 (2006) 195–202. https://doi.org/10.1016/j.memsci.2005.10.029

[11] L.M. Robeson, The upper bound revisited, J. Membr. Sci. 320 (2008) 390-400. https://doi.org/10.1016/j.memsci.2008.04.030

[12] P. D. Sutrisna, J. Hou, H. Li, Y. Zhang, V. Chen, Improved operational stability of Pebax-based gas separation membranes with ZIF-8: A comparative study of flat sheet and composite hollow fibre membranes, J. Membr. Sci. (2017) 266-279. https://doi.org/10.1016/j.memsci.2016.11.048

[13] Q. Song, S. K. Nataraj, M. V. Roussenova, J. C. Tan, D. J. Hughes, W. Li, P. Bourgoin, M. A. Alam, A. K. Cheetham, S. A. Al-Muhtasebd, E. Sivaniah, Zeolitic imidazolate framework (ZIF-8) based polymer nanocomposite membranes for gas separation, Energy Environ. Sci., 2012, 5, 8359–8369. 10.1039/c2ee21996d

[14] G. Dong, H. Li, V. Chen, Challenges and opportunities for mixed-matrix membranes for gas separation, J. Mater. Chem. A, 2013, 1, 4610–4630. 10.1039/c3ta00927k

[15] H. Bux, F. Liang, Y. Li, J. Cravillon, M. Wiebcke, J. Caro, Zeolitic imidazolate framework membrane with molecular sieving properties by microwave-assisted solvothermal synthesis, J. Am. Chem. Soc. 131 (44) (2009) 16000 − 16001. https://doi.org/10.1021/ja907359t

[16] M.J.C. Ordoñez, K.J. Balkus, J.P. Ferraris, I.H. Musselman, Molecular sieving realized with ZIF-8/Matrimid® mixed-matrix membranes, J. Membr. Sci. 361 (1−2)

(2010) 28–37. https://doi.org/10.1016/j.memsci.2010.06.017

[17] X. Liu, Y. Li, Y. Ban, Y. Peng, H. Jin, W. Yang, K. Li, Synthesis of zeolitic imidazolate framework nanocrystals, Mater. Lett. 136 (2014) 341 – 344. https://doi.org/10.1016/j.matlet.2014.08.058

[18] A. Phan, C.J. Doonan, F.J. Uriberomo, Synthesis, structure, and carbon dioxide capture properties of zeolitic imidazolate frameworks, Acc. Chem. Res. 43 (1) (2010) 58–67. https://doi.org/10.1021/ar900116g

[19] E.M. Mahdi, J.-C. Tan, Mixed-matrix membranes of zeolitic imidazolate framework (ZIF-8)/Matrimid nanocomposite: thermo-mechanical stability and viscoelasticity underpinning membrane separation performance, J. Membr. Sci. 498 (2016) 276–290. https://doi.org/10.1016/j.memsci.2015.09.066

[20] E.M. Mahdi, J.-C. Tan, Dynamic molecular interactions between polyurethane and ZIF-8 in a polymer-MOF nanocomposite: microstructural, thermo-mechanical and viscoelastic effects, Polym. 97 (2016) 31–43. https://doi.org/10.1016/j.polymer.2016.05.012

[21] B. Zornoza, B. Seoane, J.M. Zamaro, Combination of MOFs and zeolites for mixed matrix membranes, Chemphyschem. 12 (15) (2011) 2678 2678-2678. https://doi.org/10.1002/cphc.201100583

[22] S.N. Wijenayake, N.P. Panapitiya, S.H. Versteeg, Surface cross-linking of ZIF-8/ polyimide mixed matrix membranes (MMMs) for gas separation, Ind. Eng. Chem.

Res. 52 (21) (2013) 6991–7001. https://doi.org/10.1021/ie400149e

[23] J. Sánchez-Laínez, B. Zornoza, S. Friebe, J. Caro, S. Cao, A. Sabetghadam, B. Seoane, J. Gascon, F. Kapteijn, C. Le Guillouzer, G. Clet, M. Daturi, C. Téllez, J. Coronas, Influence of ZIF-8 particle size in the performance of polybenzimidazole mixed matrix membranes for pre-combustion CO_2 capture and its validation through interlaboratory test, J. Membr. Sci. 515 (2016) 45–53. 10.1016/j.memsci.2016.05.039

[24] F. V. I. Bondar, B. D. Freeman, I. Pinnau, Gas Transport Properties of Poly(ether-b-amide) Segmented Block Copolymers, J. Polym. Sci.: Part B: Polymer Physics, Vol. 38, 2051-2062 (2000). https://doi.org/10.1002/1099-0488(20000801)38:15<2051::AID-POLB100>3.0.CO;2-D

[25] A.Jomekian, R.M.Behbahani, T.Mohammadi, A.Kargari, Utilization of Pebax 1657 as structure directing agent in fabrication of ultra-porous ZIF-8, J. Solid. State. Chem. 235 (2016) 212–216. https://doi.org/10.1016/j.jssc.2016.01.004

[26] K. Kida, M. Okita, K. Fujita, S. Tanaka, Y. Miyake, Formation of high crystalline ZIF-8 in an aqueous solution, Cryst. Eng. Comm. 2013,15, 1794-1801. 10.1039/C2CE26847G

[27] Y. Zhang, Y. Jia, M. Li, L. Hou, Influence of the 2-methylimidazole/zinc nitrate hexahydrate molar ratio on the synthesis of zeolitic imidazolate framework-8 crystals at room temperature, Sci. Rep. volume 8, Article number: 9597 (2018). 10.1038/s41598-018-28015-7

[28] S. Wang, Y. Liu, S. Huang, H. Wu, Y. Li, Z. Tian, Z. Jiang, Pebax–PEG–MWCNT hybrid membranes with enhanced CO_2 capture properties, J. Membr. Sci. 460 (2014) 62–70. https://doi.org/10.1016/j.memsci.2014.02.036

[29] K.S. Park, Z. Ni, A.P. Côté, J.Y. Choi, R. Huang, F.J. Uribe-Romo, H.K. Chae, M. O'Keeffe, O.M. Yaghi, Exceptional chemical and thermal stability of zeolitic imidazolate frameworks, Proc. Natl. Acad. Sci. 103 (2006) 10186–10191. 10.1073/pnas.0602439103

[30] J. H. Kim, S.Y. Ha, Y. M. Lee, Gas permeation of poly(amide-6-b-ethylene oxide) copolymer, J. Membr. Sci. 190 (2001) 179-193. https://doi.org/10.1016/S0376-7388(01)00444-6

[31] A. Ghadimi, M. Amirilargani, T. Mohammadi, N. Kasiri, B. Sadatnia, Preparation of alloyed poly(ether block amide)/poly(ethylene glycol diacrylate) membranes for separation of CO_2/H_2 (syngas application), J. Membr. Sci. 458 (2014) 14–26. https://doi.org/10.1016/j.memsci.2014.01.048

[32] I.J.W. Bowman, D.S. Brown, R.E. Wetton, Crystal density, crystallinity and heat of fusion of poly (tetramethylene oxide), J. Polym. Sci. 10 (1969) 715-718. http://lps3.doi.org.libproxy.snu.ac.kr/10.1016/0032-3861(69)90097-4

[33] I. Pleșa, P. V. Noțingher, S. Schlögl, C. Sumereder, M. Muhr, Properties of Polymer Composites Used in High-Voltage Applications, Polym. 8 (2016) 173. 10.3390/polym8050173

[34] A. Jomekian, R.M. Behbahani, T. Mohammadi, A. Kargari, CO_2/CH_4 separation by high performance co-casted ZIF-8/Pebax 1657/PES mixed matrix membrane, J. Nat. Gas. Sci. Eng. 31 (2016) 562–574. https://doi.org/10.1016/j.jngse.2016.03.067

[35] G. Choudalakis, A. D. Gotsis, Free volume and mass transport in polymer nanocomposites, Curr. Opin. Collid & Interface. Sci. 17 (2012) 132-140. https://doi.org/10.1016/j.cocis.2012.01.004

[36] M. H. Cohen, D. Turnbull, Molecular transport in liquids and glasses, J. Chem. Phys. 31 (1959) 1164-1169. https://doi.org/10.1063/1.1730566

[37] H. Cong, M. Radosz, B. F. Towler, Y. Shen, Polymer-inorganic nanocomposite membranes for gas separation, Sep. Purif. Technol. 55 (2007) 281-291. https://doi.org/10.1016/j.seppur.2006.12.017

[38] N. K. Acharya, P. K. Yadav, Study of temperature dependent gas permeability for polycarbonate membrane, Indian J. Pure & Appl. Phys. 42 (2004) 179-181.

[39] M. Rahman, V. Filiz, S. Shishatskiy, C. Abetz, S. Neumann, S. Bolmer, M. M. Khan, V. Abetz, PEBAX® with PEG functionalized POSS as nanocomposite membranes for CO_2 separation, J. Memb. Sci. 437 (2013) 286-297. https://doi.org/10.1016/j.memsci.2013.03.001

[40] A. Jomekian, R.M. Behbahani, T. Mohammadi, A. Kargari, CO_2/CH_4 separation by high performance co-casted ZIF-8/Pebax 1657/PES mixed matrix membrane, J. Nat. Gas. Sci. Eng. 31 (2016) 562–574. https://doi.org/10.1016/j.jngse.2016.03.067

[41] J. C. Chen, X. Feng, Gas Permeation Through Poly(Ether-b-amide) (PEBAX 2533) Block Copolymer Membranes, Sep. Sci. Technol. 39 (2004) 149-164. https://doi.org/10.1081/SS-120027406